

CrystEngComm

Accepted Manuscript



This is an *Accepted Manuscript*, which has been through the Royal Society of Chemistry peer review process and has been accepted for publication.

Accepted Manuscripts are published online shortly after acceptance, before technical editing, formatting and proof reading. Using this free service, authors can make their results available to the community, in citable form, before we publish the edited article. We will replace this *Accepted Manuscript* with the edited and formatted *Advance Article* as soon as it is available.

You can find more information about *Accepted Manuscripts* in the [Information for Authors](#).

Please note that technical editing may introduce minor changes to the text and/or graphics, which may alter content. The journal's standard [Terms & Conditions](#) and the [Ethical guidelines](#) still apply. In no event shall the Royal Society of Chemistry be held responsible for any errors or omissions in this *Accepted Manuscript* or any consequences arising from the use of any information it contains.

Cite this: DOI: 10.1039/c0xx00000x

www.rsc.org/xxxxxx

ARTICLE TYPE

In-situ fabrication of Cu₂ZnSnS₄ nanoflake thin films on both rigid and flexible substrates

Xuezheng Zhai^{1,2}, Huimin Jia¹, Yange Zhang¹, Yan Lei¹, JieWei^{1,2}, Yuanhao Gao¹, Junhao Chu², Weiwei He^{1,3}, Jun-jie Yin³, Zhi Zheng^{1*}

¹Key Laboratory of Micro-Nano Materials for Energy Storage and Conversion of Henan Province and Institute of Surface Micro and Nano Materials, Xuchang University Henan 461000, China

²Key Laboratory of Polar Materials and Devices, Ministry of Education. Department of Electronics, East China Normal University. 500 Dongchuan Road, Shanghai 200241, China

³Center for Food Safety and Applied Nutrition, U.S. Food and Drug Administration, College Park, MD 20740, USA

Received (in XXX, XXX) Xth XXXXXXXXXX 200X, Accepted Xth XXXXXXXXXX 200X

DOI: 10.1039/b000000x

Cu₂ZnSnS₄ (CZTS) thin film, a highly promising and low-cost absorber layer material for solar cells, have been *in-situ* fabricated on stainless steel and FTO glass substrates for the first time using a one-step solvothermal treatment of CuZnSn-alloyed film with sulphur or selenium powder. The resulting products were characterized by X-ray diffraction (XRD), scanning electron microscopy (SEM), transmission electron microscopy (TEM), and UV-vis spectroscopy. Raman spectroscopy was used to characterize and confirm the formation of CZTS. The effects of temperature, reaction time, the ratio of Cu/Zn/Sn, and non-elemental sources on the formation of CZTS nanocrystal films were assessed, and we found that reaction temperature was a key factor in the final products. Pure CZTS phase forms at temperature 250 °C or higher. Our method produces CZTS thin films at 250°C, the lowest reaction temperature that can be used in the process and the lowest temperature of any current fabrication system. We also found that flexible substrates promote the growth of CZTS nanocrystals. Using flexible substrates in the *in-situ* fabrication of nanocrystal thin films may make it possible to use CZTS for industrial applications.

Introduction

Cu(In,Ga)Se₂ (CIGS) is regarded as one of the best absorber materials for sustainable and efficient solar cells, especially when it is compared to traditional, silicon-based solar cell materials. Currently, the maximum efficiency of the best CIGS thin-film solar cell is around 20%,¹⁻⁴ but it is expensive to produce because the gallium and indium used in the active layer are both rare and costly (indium and gallium are 0.05 ppm or less of the earth's crust).⁵ This means that large-scale production of CIGS solar cells is not cost effective. CIGS also uses toxic elements like Cd and Se, which can lead to environmental problems.

Alternative materials are expected to overcome these problems, and Cu₂ZnSnS₄ (CZTS) could be the ideal alternative for low-cost absorber layers. CZTS is a I₂-II-IV-VI₄ quaternary compound semiconductor and substitutes sulfur for the selenium, and zinc and tin for the indium, in the CIS ternary compound. All the elements used in CZTS are abundant in the earth's crust (Cu: 50 ppm, Zn: 75 ppm, Sn: 2.2 ppm, S: 260 ppm)⁵ and their toxicity is extremely low. CZTS has a direct band gap energy of 1.0–1.5

eV and a large absorption coefficient of over 10⁴ cm⁻¹, which is similar to CIGS.⁶⁻¹⁰ According to the photon balance calculations of Shockley-Queisser, CZTS has a theoretical efficiency of 32.2%,¹¹ so using CZTS films in the absorber layers of solar cells has excellent industrial possibilities.

During the past several years, interest in the design and preparation of CZTS has increased significantly because of its special crystal structure. Physical vapor and chemical deposition methods are widely used in the preparation of CZTS powders. The physical vapor method relies heavily on vacuum atmosphere, which may result in relatively low material utilization and difficulties with large-scale production.¹² The chemical deposition method involves the sulfurization of electrochemically deposited metal precursors,¹³ and sol-gel spin-coated deposition.¹⁴ These methods produce CZTS films that often contain unidentified impurities and need high-temperature annealing. Chemical deposition was developed to process large-area substrates in high throughput situations and results in high material utilization. For example, Todorov et al. fabricated CZTS thin film solar cells with 9.6% power conversion efficiency

(PCE) using a hydrazine-based hybrid slurry approach.^{15,16} Unfortunately, hydrazine is a highly toxic and very unstable compound that requires extremely careful handling and storage. This limits the applications of the method.

We developed a non-toxic, mild, ethanol-based way to fabricate dense CZTS and CZTSe thin films as absorber layers for photovoltaic applications using a one-step solvothermal treatment of the CuSnZn alloy layer (or layered elemental Cu/Sn/Zn) plus sulfur/selenium powder in the presence of absolute ethanol. Our new method has several advantages. First, CZTS and CZTSe thin films can be directly fabricated on both flexible and rigid substrates on a large scale, and the thickness of the films can be well controlled. Second, the synthesizing temperature of about 250°C is the lowest possible temperature that will form pure-phase CZTS and CZTSe thin films. Third, absolute alcohol is the only solvent that will not harm the environment. Flexible CZTS thin films prepared using our new method produce low-cost, high-efficiency, roll-to-roll flexible photovoltaic cells.

Experimental Section

Sample preparation

All reagents were analytically pure and were used as received without further purification. The substrates were cleaned with successive ultrasound baths of acetone/deionized water/isopropanol. This step ends with the substrate being dried in air at 60°C for 1 h. The CuSnZn alloy layer was deposited in an Ar atmosphere with an operating pressure of 7×10^{-3} mbar. The alloy target were applied using the stoichiometric ratio of Cu:Zn:Sn = 2:1:1, which resulted in a target purity of 99.99%. In situ monitoring of layer thickness was performed by a film thickness monitor that uses a quartz crystal. The substrate with alloy layer was put into a 25 mL PLL-lined autoclave that contained 15 mL absolute alcohol. The autoclave was sealed and run at 230–270°C for different time, then cooled to room temperature naturally. The metallic precursor thickness was 400 nm and the amount of S powder (or Se powder) was 0.01 g. The product was washed several times with absolute ethanol and then dried under room temperature for characterization.

Characterization

An X-ray diffractometer (XRD, Bruker D8 Advance) characterized the structure of the sample using nickel-filtered Cu-K α radiation at 40 kV voltage and 40 mA current. All the XRD measurements were performed within $20^\circ \leq 2\theta \leq 60^\circ$. Scanning electron microscopy (SEM, Hitachi S-4800 and Zeiss-EVO LS-15) and atomic force microscopy (AFM, Veeco Digital Instruments, Nanoscope IIIa) were used to characterize the morphology of the product. The selected area electron diffraction (SAED) patterns and the high-resolution transmission electron microscopy (HRTEM) images were captured by a JEM-2100 transmission electron microscope. Raman spectra were obtained under a 532 nm laser (Renishaw Via Raman Microscope Raman system). The UV-vis-NIR absorption spectra of as-prepared products were recorded on a Varian Cary 5000 UV-vis-NIR spectrophotometer.

Results and Discussion

Formation of the CZTS nanoflake thin films

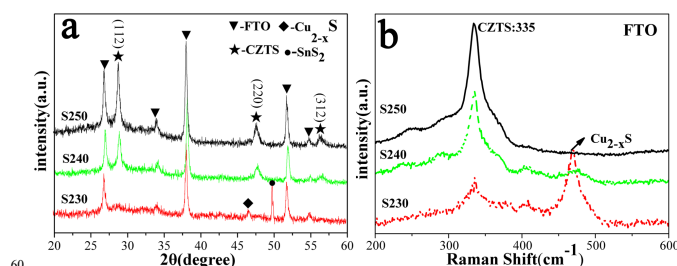


Fig. 1 (a) X-Ray diffraction patterns of the samples prepared for 18 h at 230°C, 240°C and 250°C on FTO substrates. (b) Raman spectra of the samples prepared for 18 h at 230°C, 240°C and 250°C on FTO substrates.

Although much previous work has described the growth of CZTS powders, only few papers have focused on the direct fabrication of CZTS thin films. In the present study, CZTS nanoflake thin films were *in-situ* fabricated on both flexible and rigid substrates using a mild and facile wet-chemical process. Forming CZTS nanoflake thin films on FTO is a good example of how to use a rigid substrate in this process.

To understand how the reaction paths of our system affect the formation of pure CZTS, we first investigated the influence of synthesis temperature on the formation of CZTS nanocrystals. The X-ray diffraction patterns and the corresponding raman spectra of as-prepared samples at different temperatures are shown in Fig. 1a and b, respectively. The X-ray diffraction patterns of the S230 sample indicated that pure CZTS could not be obtained at 230°C, because of the presence of binary Cu_{2-x}S and SnS₂ at 46.5° (JCPDS No. 2-1292) and 49.9° (JCPDS No. 40-1467). When the temperature was increased to 240°C or higher, pure CZTS crystals formed (curves S240 and S250). The diffraction patterns of samples obtained at 240°C and 250°C could be indexed to the pure kesterite phase of Cu₂ZnSnS₄ with three characteristic peaks at 28.5°, 47.3°, and 56.2° (JCPDS No. 26-575), which were assigned to diffraction of the (112), (220) and (312) planes. Actually, from the above XRD results, we could only estimate that 240°C is the lowest temperature at which pure CZTS crystals will form in our solvothermal system, because ZnS and Cu₂SnS₃ have very similar XRD patterns with Kesterite-type CZTS. We needed another analytical method to confirm the presence of pure CZTS phase.

Raman spectroscopy is commonly used to characterize material structures. In thin film materials, XRD techniques are difficult to detect if the film material doesn't have a good crystallinity. When Raman spectroscopy was used to test the microcrystalline group effect of chalcogenide compounds, the presence of SnS with characteristic modes at 160 cm⁻¹, 190 cm⁻¹, 220 cm⁻¹, and SnS₂ with modes at 315 cm⁻¹ was reported by Parkin et al.¹⁷ The major peaks at 475 cm⁻¹, 304 cm⁻¹ and 356 cm⁻¹ corresponded to Cu_{2-x}S,¹⁸ Sn₂S_{3,¹⁷ and ZnS.¹⁹ The major peaks at 318 cm⁻¹, 348 cm⁻¹, and 295 cm⁻¹ corresponded to Cu₃SnS_{4.⁴}}

Raman techniques have recently been used by a number of researchers to confirm the formation of pure CZTS. There have been many reports on the raman peak position of CZTS,

including a typical peak at 333 cm^{-1} and a weak shoulder at 284 cm^{-1} . Raman peaks at $338\text{--}339\text{ cm}^{-1}$, 288 cm^{-1} , and $256\text{--}257\text{ cm}^{-1}$ were reported by P. A. Fernandes,² and peaks at 286 cm^{-1} , 328 cm^{-1} , and 367 cm^{-1} were reported by H. Katagiri.²² Other researchers have found CZTS Raman peaks at $\sim 252\text{ cm}^{-1}$, $\sim 287\text{ cm}^{-1}$, $\sim 338\text{ cm}^{-1}$, $\sim 351\text{ cm}^{-1}$, and $\sim 368\text{ cm}^{-1}$, with the strongest peak at $\sim 338\text{ cm}^{-1}$.^{20,21} The migration phenomenon associated with these peaks was produced because CZTS exists within a small stoichiometric range. There is no official or standard assignment of active Raman peaks for CZTS films at the current time.

We examined all prepared samples with Raman spectroscopy. Fig. 1b shows the Raman spectra for samples S230, S240, and S250 with 532 nm laser excitation. The characteristic peak we found at 335 cm^{-1} from the curve S250 matches the results of previous research,⁴ and indicated the presence of pure CZTS nanocrystals. No other characteristic peaks of impurities were observed. The Raman signals of CZTS (335 cm^{-1}) and Cu_{2-x}S (475 cm^{-1}) were both detected in curve S230 (Fig. 1b). The peak intensity of Cu_{2-x}S decreased while the peak intensity of CZTS increased with the increase of temperature (S240), which indicated that higher temperatures make the hydrothermal reaction more thorough and promote the binary and ternary phase change into CZTS.

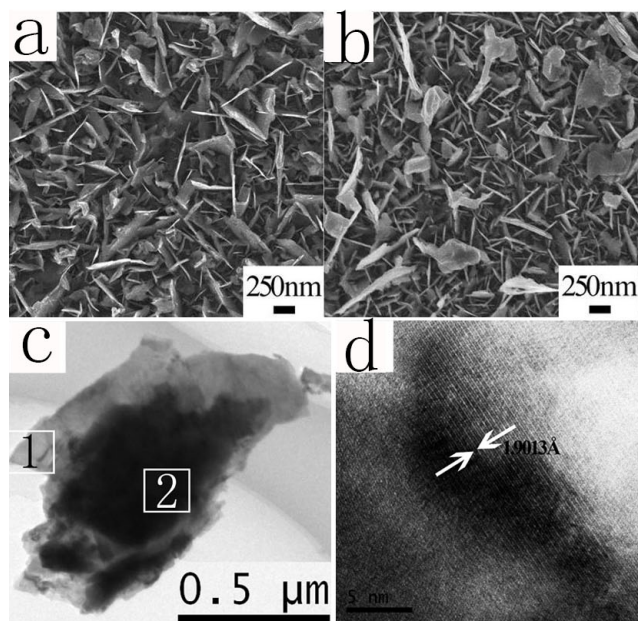


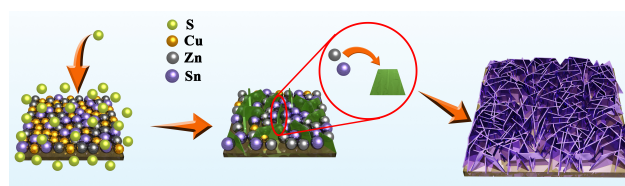
Fig. 2 SEM images of the CZTS nanocrystalline thin films prepared at 250°C for 6 h (a) and 18 h (b). (c) TEM image of an individual CZTS nanoflake. (d) The HRTEM images taken from rectangle frame 1 of the nanoflakes.

From the XRD and Raman results, we concluded that 250°C is the lowest temperature for forming pure CZTS crystals in our solvothermal system. The CZTS crystals that formed at 230°C had impurities, and XRD could not detect CZTS because of their inferior crystallinity. When the temperature increased, the crystallinity improved and more CZTS was found. The complicated reaction process is not discussed here.

Fig. 2a and 2b show the typical SEM images of the as-prepared CZTS films obtained at 250°C for 6 h and 18 h, respectively. The

CZTS films were composed of plenty of nanoflakes perpendicular to the surface of the FTO glass substrate. There was a clear hierarchy of thicker flakes at the top that transitioned to thinner flakes at the bottom with an average thickness of $\sim 20\text{ nm}$. As the reaction time extended, relatively dense nanoflakes were formed (Fig. 2b). Fig. 2c displays the TEM image of an individual CZTS nanoflake obtained after an ultrasonic dispersal treatment of the CZTS sample. It shows the fracture surface of the broken CZTS nanoflake. High-resolution transmission electron microscopy images of nanoflakes (Fig. 2d) taken from rectangle frame 1 are shown in Fig. 2c. Rectangle frame 2 is superposed nanoflakes. In rectangle frame 1, we can clearly see the lattice fringes with an interplanar spacing of 1.9013 \AA that can be assigned to the (220) plane of CZTS. These results indicate that individual nanoflakes are single-crystalline.

We hypothesized that, since the reaction of elemental sulfur with copper is faster than the reaction of tin with zinc, the copper ions combine with the sulfide ions and make CuS on the surface of the crystal along the preferential direction (scheme 1a). This produces copper vacancies.^{23,24} The tin and zinc ions enter the internal structure of the crystal and occupy the spaces left by the departed copper (scheme 1b). The growth of sheet-like CZTS crystals relies strongly on the crystal structure of CuS nanoflakes. They eventually cover the nanoflake film completely (scheme 1c). The schematic diagram of the formation mechanism of CZTS thin films on the substrates with sulphur powder is as shown in scheme 1.



Scheme 1. The schematic diagram of the formation mechanism of CZTS thin films.

The influence of substrate on the crystallization of CZTS

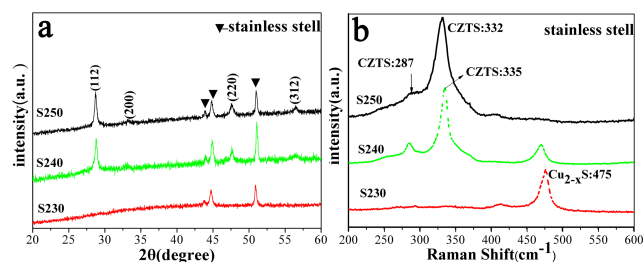


Fig. 3 (a) X-Ray diffraction patterns of the samples prepared for 18 h at 230°C , 240°C and 250°C on stainless steel substrates. (b) Raman spectra of the samples prepared for 18 h at 230°C , 240°C and 250°C on stainless steel substrates.

Stainless steel materials were used in our research because they are dependably flexible and can be used in cost-effective, large-scale industrial applications. Researchers have synthesized CZTS on rigid substrates in many different ways, but few people have studied the fabrication of CZTS on flexible substrates. We tried to use rigid substrate methods to directly synthesize CZTS

crystals on stainless steel flexible substrates so the results would be useful for industrial applications. Fig. 3 shows the X-ray diffraction patterns of the as-prepared products obtained at various reaction temperatures on stainless steel substrates. The X-ray diffraction patterns only showed the presence of the stainless steel substrate in the S230 curve (Fig. 3a). No CZTS peaks were detected. However, the existence of Cu_{2-x}S was confirmed by the presence of a Raman peak at 475 cm^{-1} in the S230 curve (Fig. 3b), indicating that the as-prepared products on stainless steel were only the binary phase Cu_{2-x}S at 230°C . At 230°C on FTO substrate, however, the binary phase (Cu_{2-x}S) and the quaternary phase (CZTS) were both formed. When the temperature increased to 240°C , the Raman signals of CZTS and Cu_{2-x}S were all detected on stainless steel (S240). The characteristic peaks of CZTS at 287 and 332 cm^{-1} in the S250 curve were consistent with the data in the literature,⁴ indicating the presence of CZTS nanocrystals.

When we compared the CZTS growth process on FTO substrates and stainless steel substrates, we found that CZTS nanocrystals formed more easily on the FTO substrates than on the stainless steel substrates under the same reaction conditions. We inferred that the surface morphology caused by magnetron sputtering may influence the growth of CZTS nanocrystals. The surface morphologies of the as-prepared CuZnSn alloy films were captured by an atomic force microscope (AFM). Fig. 4a and 4b show the two-dimensional AFM images of a CuZnSn alloy film deposited by magnetron sputtering on stainless steel and FTO glass substrates, respectively. The average grain sizes of CuZnSn alloy nanoparticles on FTO were $80\text{--}150\text{ nm}$ with high density (Fig. 4b), but the surface morphology of CuZnSn alloy film on a stainless steel substrate was irregular. This large difference in initial CuZnSn gains morphology may affect the reaction kinetics that form CZTS on different substrates. The exact mechanism needs further investigation.

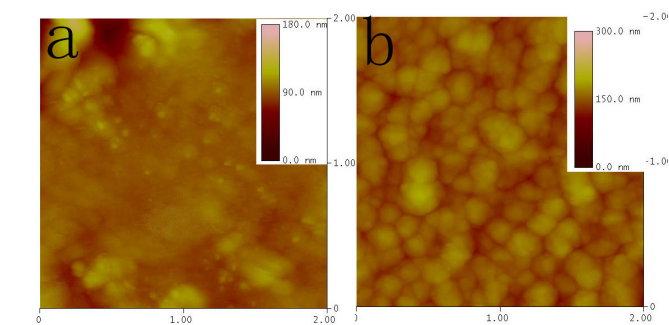


Fig. 4 (a) AFM images of the original CuZnSn alloy layer on stainless steel surfaces and (b) on FTO surfaces.

The influence of composition on the crystallization of CZTS on FTO substrates

A uniform alloy layer was easily obtained using alloy targets from magnetron sputtering, but it was difficult to tune the ratio of metal elements and study the effect of composition on the formation of CZTS films. The layer-by-layer sputtering method was used to control the ratio of various elements. Sn, Cu and Zn were successively sputtered onto the FTO substrates. The purity of all target materials was 99.99%. Individual thicknesses were estimated using the density and molecular weight of each element.

Trimetallic CuSnZn films with Cu/Sn/Zn ratios of 2:1:1, 1.5:1:1 and 1:1:1 were formed, then reacted with S powder to prepare CZTS. Fig. 5 shows the Raman spectroscopy results of the CZTS film obtained at 250°C for 18 h on FTO substrates, in which the main CZTS peak shifts from 331 cm^{-1} to 335 cm^{-1} as the proportion of origin copper increases. The XRD patterns in Fig. 1 and the Raman spectra patterns in Fig. 3 showed copper combining with S powder to form copper sulfide (Cu_{2-x}S), and tin and zinc ions entering the internal crystal to occupy copper vacancies and form CZTS. The proportion of copper was a critical factor in the synthesis of CZTS, and the increased Cu content in the original metal film induced crystal structure variations in final CZTS films, which led to a Raman peak shift. This Raman shift may be related to d-spacing or compressive stress in sprayed films.²⁰

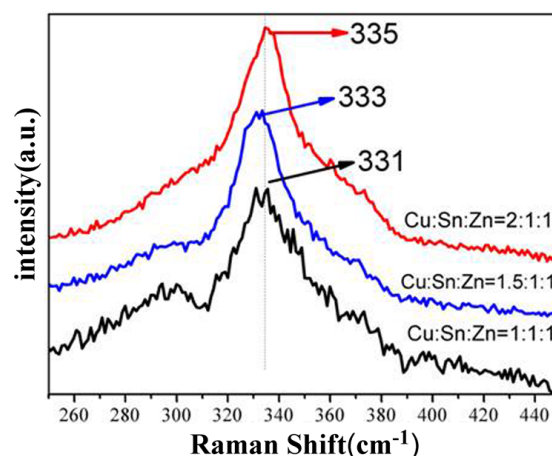


Fig. 5 Raman images of the CZTS nanocrystalline thin films prepared at 250°C for 18 h.

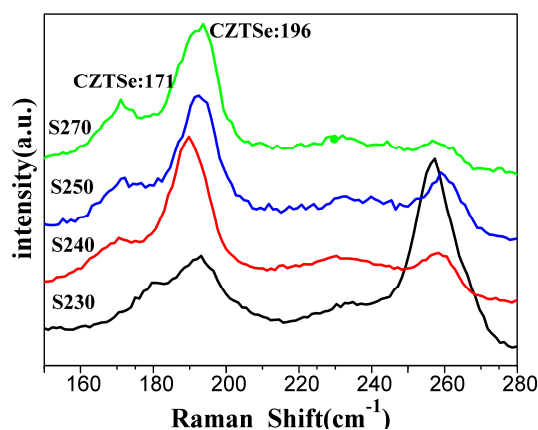


Fig. 6 Raman spectra of the CZTSe nanocrystalline thin film samples prepared for 18 h on stainless steel substrates. The reaction temperatures were 230°C , 240°C , 250°C , and 270°C .

Influence of non-elemental reactants on the crystallization of CZTS(Se)

Se and S are elements of the same family and have similar natures, so we attempted to synthesize a CZTSe film with CZTS methods, using Se powder instead of S powder. The effects of

temperature and time on crystal growth were studied using Raman spectroscopy. The effect of reaction temperature on CZTSe formation was investigated by fixing the thickness of the CuZnSn film (400 nm) and the reaction time (18 h and 24 h). Fig. 6 shows the Raman spectra of the CZTSe nanocrystals obtained at various reaction temperatures on stainless steel substrates. The Raman spectra revealed the presence of Cu_xSe_y (260 cm^{-1}) and CZTSe ($196, 172\text{ cm}^{-1}$) at 230°C . When the reaction temperature increased, we found that the peak intensity of Cu_xSe_y at 260 cm^{-1} diminished but the peak intensity of CZTSe at 196 cm^{-1} increased considerably. The peaks of Cu_xSe_y disappeared when the selenide temperature increased to 270°C . We hypothesized that the pure CZTSe crystal may form at 270°C because the higher reaction temperature made the reaction more thorough.

The effect of reaction time was also tested. Fig. 7 shows the Raman spectra of the CZTSe nanocrystal obtained at 250°C on stainless steel substrates for different reaction times. Raman spectra derived from CZTSe formed at 24 h shows typical peaks at 196 and 172 cm^{-1} without evidence of Cu_xSe_y raman signals. We compared it to the CZTSe film obtained at 18 h and concluded that a longer reaction time promotes the growth of pure CZTSe in hydrothermal conditions, and changing the hydrothermal reaction temperature and reaction time is an effective way to fabricate high yield CZTSe films without impurities.

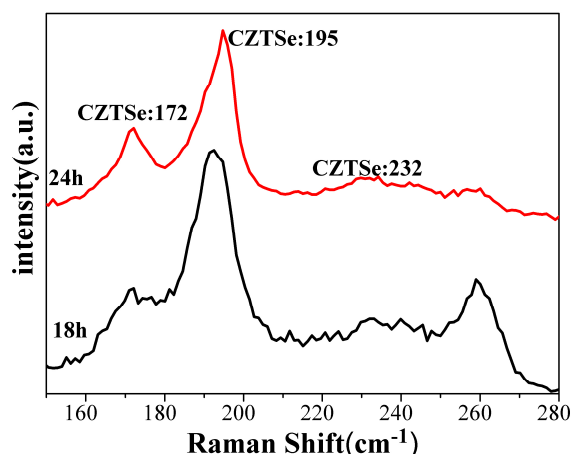


Fig. 7 Raman spectra of CZTSe nanocrystalline thin film samples prepared at 250°C on stainless steel substrates. The reaction times were 18 h and 24 h.

Optical properties of the as-prepared CZTS nanoflake thin films

Fig. 8 shows the absorption spectra of CZTS nanoflake thin films prepared at 250°C for 18 h. The films have a wide absorption wavelength range, from visible light (400 nm) to near the infrared region (1100 nm). Due to direct forbidden reactions, the absorption characteristics of the as-prepared sample obey the model equation $(\alpha h\nu)^2 = A(h\nu - E_g)$, where α is the optical absorption coefficient, h the Planck constant, ν the photon frequency, A a constant, and E_g the energy gap. The extrapolated value (the straight line to the x-axis) of $h\nu$ at 0 gives the absorption band gap E_g corresponding to 1.45 eV (inset of Fig. 8). The calculated band gap of CZTS nanoflake thin films is in agreement with the reported values of 1.0-1.5 eV²⁵⁻²⁷. The

UV-vis-NIR absorption spectra and the corresponding $(\alpha h\nu)^2$ vs. $h\nu$ curve of the CZTS thin film prepared at different temperatures and different time were shown in Figure S6 and Figure S7. We found that the absorption edge of the sample prepared at 230°C and 240°C shifted to the short wavelength direction, comparing with the sample prepared at 250°C . This phenomenon can be explained by the absorption of Cu_{2-x}S or SnS_2 at 230°C and 240°C . The results are corresponding to the previous XRD and Raman data. Also, the reaction time is an important factor for the synthesis of CZTS thin film. The absorption edge of the as-prepared CZTS thin films for 6 h shifted to the short wavelength direction, which ascribe to the absorption of Cu_{2-x}S . The changes of absorption curves of the sample prepared for 18 h and 24 h were not obvious. This phenomenon is consistent with the previous results.

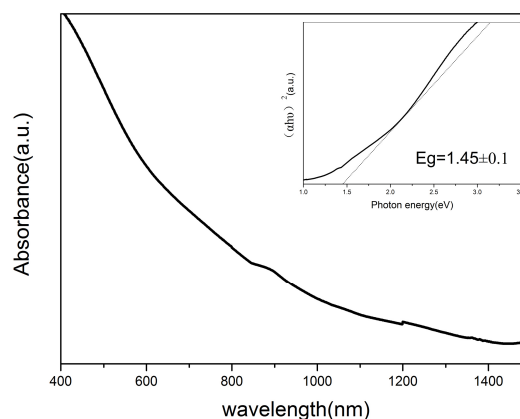


Fig. 8 UV-vis-NIR absorption spectra of the CZTS thin film prepared at 250°C for 18 h. The inset is the corresponding $(\alpha h\nu)^2$ vs. $h\nu$ curve.

Conclusions

In conclusion, CZTS nanocrystal thin film absorber layers have been successfully *in situ* fabricated on both flexible stainless steel and rigid FTO substrates using a non-toxic, mild, and solvothermal process. The thickness of the films was well controlled. The effect of synthetic conditions, such as reaction temperature, reaction time, substrates and the composition of metal films on the morphology and crystalline phase of CZTS were discussed systematically and reaction temperature was found to play a critical role in the formation of the final products. When we used the method we developed, we discovered that pure CZTS phase could only be obtained at temperatures of 250°C or higher, but the lowest temperature of any current fabrication system reported. Our fabrication system also cost less, covered more area, and was more environmentally friendly than the other known methods. It provides a low temperature way to prepare CZTS thin film for photovoltaic applications, and its use of flexible substrates will make large-scale industrial applications of CZTS thin films possible.

Acknowledgments

We thank Barbara Berman from U.S. FDA for her kind and scientific editing. This work was supported by the National

Natural Science Foundation of China (Grant No. 21273192, 61204009), the Innovation Scientists and Technicians Troop Construction Projects of Henan Province (Grant No. 144200510014), the Program for Science & Technology Innovation Teams in the Universities of Henan Province (2012 IRTSTHN021), the Innovation Scientists and Technicians Team Projects of Henan Province Program for Basic and Advanced Technology of Henan Province (Grant No. 112300410106, 124300510055), and the Research Key Projects of Science and Technology of Henan Province (Grant No. 12A150022).

- 24 Y. Lei, H.M. Jia, Z. Zheng, Y.H. Gao, X.W. Chen and H.W. Hou, *Cryst. Eng. Comm.*, 2011, **13**, 6212–6217.
25 F. J. Fan, L. Wu, M. Gong, G. Y. Liu, Y. X. Wang, S. H. Yu, S. Y. Chen, L.W. Wang and X. G. Gong, *ACS nano*, 2013, **7**, 1454–1463.
70 26 H. R. Yang, L. A. Jauregui, G. Q. Zhang, Y. P. Chen, and Y. Wu, *Nano Lett.*, 2012, **12**, 540–545.
27 X. Z. Lin, J. Kavalakkatt, K. Kornhuber, S. Levcenko, M. Lux-Steiner and A. Ennaoui, *Thin Solid Films*, 2013, **535**, 10–13.

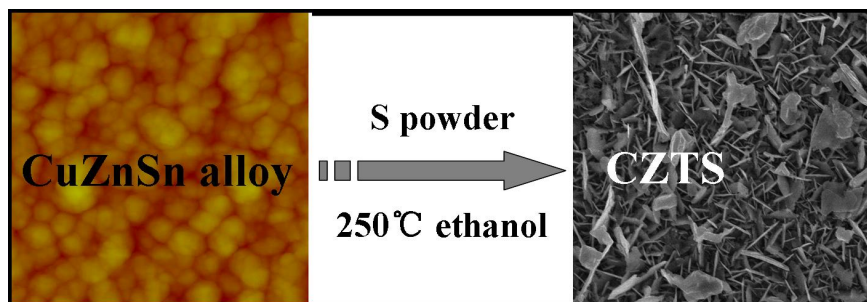
Notes and references

^a Key Laboratory for Micro-Nano Energy Storage and Conversion

15 Materials of Henan Province, Institute of Surface Micro and Nano Materials, Xuchang University, Henan 461000, P. R. China. Fax: +86-374-2968988; Tel: +86-374-2968988; Email:zhengzhi99999@gmail.com

- 20 1 A. Fischereder, T. Rath, W. Haas, H. Amenitsch, J. Albering, D. Meischler, S. Larissegger, M. Edler, R. Saf, F. Hofer and G. Trimmel, *Chem. Mater.*, 2010, **22**, 3399–3406.
2 P. A. Fernandes, P.M.P. Salomé, A.F. da Cunha, *Thin Solid Films*, 2009, **517**, 2519–2523.
25 3 C. Steinhagen, G. Matthew, V.A. Panthani, B. Kool and B.A. Korgel, *J. Am. Chem. Soc.*, 2009, **131**, 12554–12555.
4 Y.L. Zhou, W.H. Zhou, M. Lei, Y.F. Du and S.X. Wu, *J. Phys. Chem.*, 2011, **115**, 19632–19639.
5 H. Katagiri, K. Jimbo, K. Oishi, M. Yamazaki, H. Araki and A. Takeuchi, *Thin Solid Films*, 2009, **517**, 2455–2460.
30 6 S.C. Riha, B.A. Parkinson and A.L. Prieto, *J. Am. Chem. Soc.*, 2009, **131**, 12054–12055.
7 V.G. Rajeshmon, C.S. Kartha, K.P. Vijayakumar, C. Sanjeeviraja, T. Abe and Y. Kashiwaba, *Solar Energy*, 2011, **85**, 249–255.
35 8 M. Cao, Y. Shen, *J. Cryst. Growth*, 2011, **318**, 1117–1120.
9 S. Ahmed, K.B. Reuter, O. Gunawan, L. Guo, L.T. Romankiw and H. Deligianni, *Energy Mater.*, 2011, 1–7.
10 K. Tanaka, Y. Fukui, N. Moritake and H. Uchiki, *Sol. Energy Mater. Sol. Cells*, 2011, **95**, 838–842.
40 11 W. Shockley and H.J. Queisser, *J. Appl. Phys.*, 1961, **32**, 510–519.
12 K. Woo, Y. Kim and J. Moon, *Energy Environ. Sci.*, 2012, **5**, 5340–5345.
13 H. Araki, Y. Kubo, A. Mikaduki, K. Jimbo, W.S. Maw, H. Katagiri, M. Yamazaki, K. Oishi, and A. Takeuchi, *Sol. Energy Mater. Sol. Cells*, 2009, **93**, 996–999.
45 14 N. Kamoun, H. Bouzouita, B. Rezig, *Thin Solid Films*, 2007, **515**, 5949–5952.
15 T.K. Todorov, K.B. Reuter and D.B. Mitzi, *Adv. Mater.*, 2010, **22**, E156–E159.
50 16 Q.J. Guo, H.W. Hillhouse and R. Agrawal, *J. Am. Chem. Soc.*, 2009, **131**, 11672–11673.
17 I.P. Parkin, L.S. Price, T.G. Hibbertb, K.C. Molloyb, *J. Mater. Chem.*, 2001, **11**, 1486–1490.
18 C.G. Muncea, G.K. Parkera, S.A. Holtb, G.A. Hopea, *Colloids Surf. A. Physicochem. Eng. Asp.*, 2007, **295**, 152–158.
55 19 J. Serrano, A. Cantarero, M. Cardona and B.A. Weinstein, *Phys. Rev. B*, 2004, **69**, 014301.
20 H. Yoo and J H. Kim, *Sol. Energy Mater. Sol. Cells*, 2011, **95**, 239–244.
60 21 A. Fairbrother, X. Fontane and V. Izquierdo-Roca, *Sol. Energy Mater. Sol. Cells*, 2013, **112**, 97–105.
22 H. Katagiri, K. Jimbo and S. Yamada, *Appl. Phys. Express*, 2008, **1**, 4, 41201–41202.
23 H. M. Jia, W.W. He, X.W. Chen, Y.Lei and Z. Zheng, *J. Mater. Chem.*, 2011, **21**, 12824–12828.

SYNOPSIS TOC



Pure CZTS thin film forms at temperature 250 °C, the lowest temperature of any current fabrication system, directly on both flexible stainless steel and rigid FTO substrates.